Observing Superradiant Decay of Excited-State Helium Atoms Inside Helium Plasma

Hui Xia,[1,2] Anatoly A. Svidzinsky,[1,2] Luqi Yuan,[2] Chao Lu,[1] Szymon Suckewer,[1] and Marlan O. Scully[1,2,3]

[1]*Princeton University, Princeton, New Jersey 08542, USA*
[2]*Texas A & M University, College Station, Texas 77843, USA*
[3]*Baylor University, Waco, Texas 76706, USA*

(Received 27 February 2012; published 30 August 2012)

Using femtosecond transient absorption spectroscopy on excited-state helium atoms in a plasma created through optical field ionization, we measured the decay of 2^3S-2^3P excitation with sub-ps temporal resolution. The population evolution shows that initial decay is significantly faster than the electron-atom collisions and three orders of magnitude faster than the single atom spontaneous decay rate. This indicates on superradiant coherent behavior of the atomic system inside the plasma.

DOI: 10.1103/PhysRevLett.109.093604 PACS numbers: 42.50.Nn, 32.80.Fb, 32.80.Qk, 42.50.Ct

In a plasma of modest to high electron density, electron-ion or electron-atom collisions are usually the dominating decoherence mechanisms limiting the effect of atomic coherence, unless coherence manifests in a time scale shorter than the collisional time. One such scenario is the cooperative spontaneous emission for an ensemble of coherently excited atoms. The process, termed as ''superradiance,'' was first described by Dicke [1] and experimentally observed by Feld and co-workers [2]. It features an enhanced spontaneous decay rate much greater than that of an isolated single atom. Superradiance is also often viewed as part of superfluorescence process in which coherence develops in initially incoherent inverted medium. Over the years both superradiance and superfluorescence have been extensively studied in a wide range of systems, including the picosecond regime time-resolved cooperative emissions in atomic vapors [3]. Recently, superfluorescence from helium atoms following excitation by free-electron laser has been observed with the aim of generation of XUV and x-ray superfluorescence pulses [4]. For tabletop systems, plasma based collisional or recombination schemes are perspective approaches for producing XUV and x-ray lasers [5], and it is of significant interest to explore whether coherence effects can be incorporated there in a suitable way.

In this Letter, we report femtosecond absorption spectroscopy measurement of the superradiant decay of helium atoms from 2^3P to 2^3S state in a plasma created through optical field ionization. Coherence between levels 2^3P and 2^3S is created by a short laser pump pulse resonant with 2^3S-2^3P transition. Evolution of the population on the 2^3P level is probed with sub-ps temporal resolution by measuring absorption of a short probe pulse resonant with 2^3P-3^3D transition that is sent with a delay. Population decay pattern shows the signature of the superradiant enhancement with a rapid decay component more than three orders of magnitude faster than the single atom decay time at density of atoms in the 2^3S state on the order of 10^{13} cm^{-3}. We also observed the effects of so-called ''perturbed free induction decay'' when the probe precedes the strong pump pulse. In such case, the phase and amplitude of the atomic polarization excited by the probe that is responsible for the coherent radiation of the 3^3D-2^3P transition is controlled by a delayed strong pump pulse that resonantly couples 2^3P and 2^3S levels. As a result, oscillations as well as significant changes appear in the collected transmission spectra of the probe pulse.

In our experiments, excited helium is prepared via optical field ionization followed by nonradiative three-body (two electrons and one ion) recombination, whose cross section is approximately proportional to the fourth power of the principal quantum number of atomic states, and collisional deexcitation. Under intense laser field, atoms are stripped off electrons through Keldysh tunneling [6]. In order for three-body recombination to dominate over radiative decay as well as collisional ionization, a plasma of low electron temperature with high initial electron density is required. With the ionization laser pulses shorter than the electron collision time, plasma heating can be minimized.

Our typical experimental setup has a glass cell of 5 cm in diameter and 30 cm long, flowed with helium at various pressures. A Ti: Sapphire femtosecond regenerative amplifier system (KMLabs) produces 50 fs pulses of central wavelength 790 nm and pulse energy of 3 mJ at a repetition rate of 1 kHz. Part of the beam is used to pump two optical parametric amplifiers (OPA, from Light Conversion, Inc.), and the remaining portion is focused into the helium cell as the ionizing beam, with peak intensity of 2×10^{15} W/cm^2. At such intensity, nearly 100% of helium atoms will be ionized at the central part of the beam. The output from the OPA is tunable in the wavelength range from 550 to 2200 nm. One of the OPA output is used as the probe beam, and is focused into the helium cell at diameter of around 50 μm. All the beams are linearly polarized and the relative delay between the beams is controlled by varying the beam optical paths.

Population of the excited levels is monitored by measuring transmission spectra of probe pulses. Figure 1(a)

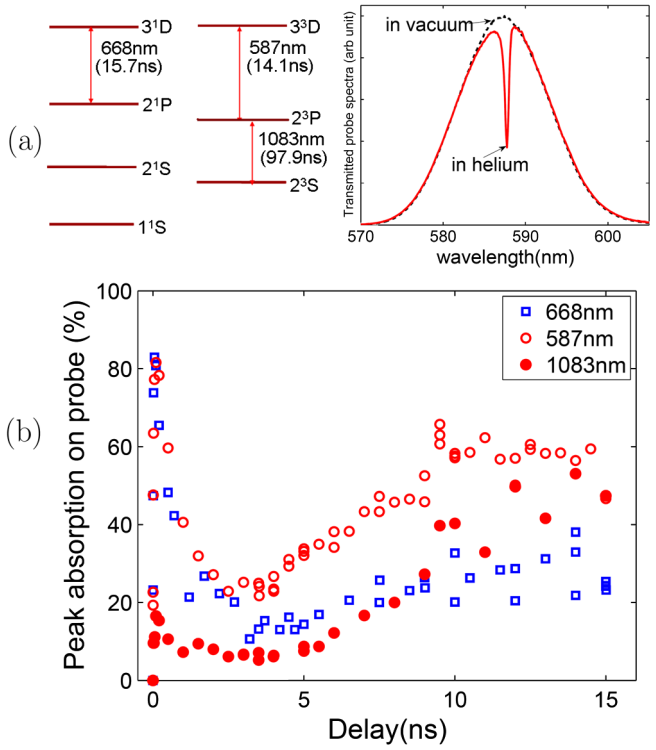

FIG. 1 (color online). (a) Energy levels of helium atom (not to scale) and the typical transmitted spectra of the probe pulse at 2^3P-3^3D (587 nm) transition sent 10 ns after helium ionization. (b) Peak absorption on the probe for 2^1P-3^1D (668 nm), 2^3P-3^3D (587 nm), and 2^3S-2^3P (1083 nm) transitions as function of probe delay after ionization pulse. The pressure of helium is 100 mbar which corresponds to the density of 2.5×10^{18} cm^{-3} of the initial neutral helium before ionization.

shows typical spectra of probe pulse transmitted through the ionized helium when its central wavelength is tuned to the resonance with 2^3P-3^3D (587 nm) transition. The probe pulse has a pulse duration of 250 fs, with an energy on the order of 1 nJ per pulse. The broad probe beam spectrum is much wider than the linewidth of the transition. Therefore, the resonant feature is shown as a dip in the transmitted spectra. Taking into appropriate account of the spectrometer resolution (in our case about 0.2 nm at wavelength of 600 nm), the absorption profile can be used to calculate the population difference between 2^3P and 3^3D levels.

Figure 1(b) shows the peak absorption on the probe beam as a function of delay for the three transitions probed [shown in Fig. 1(a)]. The HeI excited states populated from the ionization and the recombination processes can be distinctly seen as the early (faster) and later (slower) components. This feature is qualitatively similar to the structures described in the emission spectroscopic measurement in Ref. [7]. The early component, on time scale less than a nanosecond, is related to the excitation of helium atoms during the ionization process, as well as the impact excitation, deexcitation, or ionization by the hot electrons right after the ionization pulse. The slower

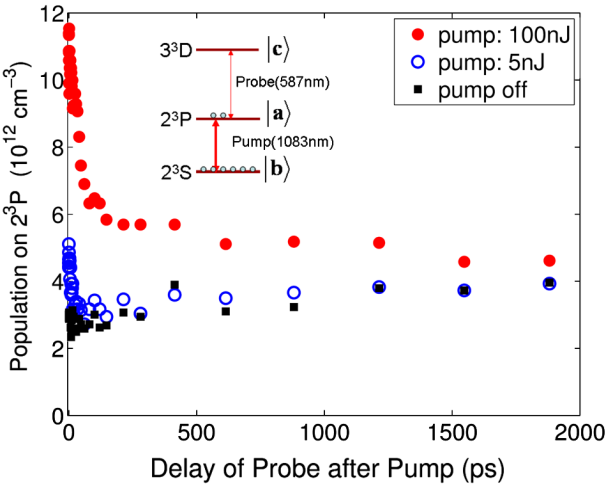

FIG. 2 (color online). Population density of 2^3P level as a function of time after pump pulse. Initial helium pressure before ionization is 25 mbar.

component is primarily attributed to the three-body-recombination process, which starts to fill the levels at time scale of several nanoseconds, and is pressure (density) and level dependent. It can also be seen that in the recombination process more absorption is observed for the triplet transition (587 nm triplet transition vs 668 nm singlet transition), which primarily is related to the higher degeneracy of states for triplet levels.

We conducted a pump-probe type of measurement of the population of the helium excited states by sending a pump beam from the output of a second OPA. The pump pulse has duration of 100 fs, a central wavelength of 1083 nm (in resonance with the 2^3S-2^3P transition), and a typical energy of 100 nJ/pulse. The probe beam is tuned to 587 nm to probe the 2^3P-3^3D transition. The time delay of the pump pulse after helium ionization is fixed at 26 ns while arrival of the probe relative to the pump pulse is varied by adjusting its optical path. Estimated from the absorption spectra, atomic densities prior to the pump pulse are 3×10^{12} cm^{-3} for 2^3P and 1.2×10^{13} cm^{-3} for 2^3S states respectively.

Figure 2 shows population density of 2^3P level obtained from the measured transmission spectra of the probe as a function of time after the pump pulse. For these data, the absorption of the probe is attributed to the population of the 2^3P state (population of 3^3D level is negligibly small as compared to those of 2^3P). For the sake of simplicity we neglected the level splittings and degeneracies, and treated each triplet level as single state. The actual population of each sublevel may be excited differently by the pump pulse. However, the average population evolution should be well described by the simplified picture. Excitation by the pump beam adds population to the 2^3P level. Probe pulse allows us to measure how 2^3P population decays back to its balanced value. The data obtained show that decay curve has a fast and slow components. At pump

energy of 100 nJ, corresponding to the pulse area of 1.1π (calibrated separately), the fast and slow components have time constants of about 50 ps and 1 ns respectively. With a weak pump of 5 nJ and pulse area of 0.25π, the fast component has shorter time constant (~ 10 ps) as compared to the case of strong pump while the slow part of the decay curve is mostly below the experimental precision level for obtaining accurate time constant.

Next we estimate the electron-atom collision rate in the plasma environment. The initial plasma density is around 6×10^{17} cm^{-3}. Plasma's volume expands after the passage of the ionization pulse. Plasma expansion can be described using shock model [7,8] in which the rate of radius expansion decreases with time as $1/\sqrt{t}$. At 26 ns after ionization, the plasma density is in range of 10^{16} to 10^{17} cm^{-3} and the electron temperature is of the order of 0.5 to 1 eV. Under such conditions the electron-atom collision time is estimated to be at least several hundred picoseconds or longer. Therefore, the observed rapidly decaying level population evolves at least one order of magnitude faster than the electron-atom collision time.

Comparing our data with theoretical model of superradiant decay upon coherent excitation, we consider a medium composed of two level atoms (the upper level a and the lower level b). Particle density n is assumed to be uniform inside the sample. A laser pulse of Rabi frequency $\Omega(t, z)$ enters the medium and propagates along the z axis. We use semiclassical approach in which evolution of $\Omega(t, z)$ is described by Maxwell's equation that in slowly varying envelope approximation reads

$$\frac{\partial \Omega}{\partial z} + \frac{1}{c}\frac{\partial \Omega}{\partial t} = i\eta\rho_{ab}, \tag{1}$$

where $\eta = 3n\lambda^2\gamma/8\pi$, λ is the wavelength of the atomic transition, and γ is the single atom spontaneous decay rate. Equation (1) is supplemented by quantum mechanical equations for the atomic density matrix

$$\dot{\rho}_{aa} = -\gamma\rho_{aa} - i(\Omega^*\rho_{ab} - c.c.), \tag{2}$$

$$\dot{\rho}_{ab} = -\frac{\gamma}{2}\rho_{ab} + i\Omega(\rho_{bb} - \rho_{aa}), \tag{3}$$

$$\rho_{aa} + \rho_{bb} = 1. \tag{4}$$

For weak excitation, one can approximate $\rho_{bb} - \rho_{aa} \approx 1$ in Eq. (3). As a result, equations for $\Omega(t, z)$ and $\rho_{ab}(t, z)$ decouple and system of Eqs. (1) and (3) can be solved analytically for arbitrary initial conditions. In the present experiment we send a very short pulse (shorter than any other characteristic time scales in the problem) which can be treated as a δ function, $\Omega(0, z) \propto \delta(z)$. For this initial condition Eqs. (1)–(4)(4) yield

$$\rho_{aa}(t, z) \propto J_0^2(2\sqrt{\eta z(t - z/c)})e^{-\gamma(t-z/c)}\theta(ct - z), \tag{5}$$

where $J_0(x)$ is the Bessel function.

In our experiment the incident short pump pulse drives the $2^3S \leftrightarrow 2^3P$ transition which has wavelength $\lambda = 1083.3$ nm and spontaneous decay time $1/\gamma = 97.9$ ns. This pulse excites atomic medium so that population of atoms in the 2^3P state is given by Eq. (5). A second weak short probe pulse resonant with the $2^3P \leftrightarrow 3^3D$ transition is sent with a delay Δt. During propagation this probe pulse sees the following population of atoms in the 2^3P state

$$\rho(z) = \rho_{aa}(t = \Delta t + z/c, z) \propto J_0^2(2\sqrt{\eta z\Delta t})e^{-\gamma\Delta t}. \tag{6}$$

Using

$$\frac{1}{L}\int_0^L J_0^2(2\sqrt{\eta z\Delta t})dz = J_0^2(2\sqrt{\Gamma_N\Delta t}) + J_1^2(2\sqrt{\Gamma_N\Delta t}), \tag{7}$$

we obtain that the integrated population seen by the second pulse after propagation through the whole sample of length L is

$$\frac{\rho(\Delta t)}{\rho(0)} = [J_0^2(2\sqrt{\Gamma_N\Delta t}) + J_1^2(2\sqrt{\Gamma_N\Delta t})]e^{-\gamma\Delta t}, \tag{8}$$

where

$$\Gamma_N = \eta L = \frac{3}{8\pi}n\lambda^2 L\gamma, \tag{9}$$

is the characteristic collective decay rate proportional to the atomic density n. If atom concentration in the 2^3S state is $n = 1.2 \times 10^{13}$ cm^{-3} and $L = 0.5$ cm then Eq. (9) gives $1/\Gamma_N = 12$ ps. This superradiant time scale is much shorter than spontaneous decay time $1/\gamma = 97.9$ ns as well as the time between collisions in our experiment. Absorption of the second pulse is proportional to the integrated population (8) of the 2^3P level, which thus can be measured as a function of time Δt lapse since the level 2^3P is excited by the first pulse. For $\Delta t \lesssim 1/\Gamma_N$ Eq. (8) yields $\rho(\Delta t) \propto e^{-(\Gamma_N+\gamma)\Delta t}$ while for $\Delta t \gg 1/\Gamma_N$ we obtain $\rho(\Delta t) \propto e^{-\gamma\Delta t}/\sqrt{\Delta t}$.

For strong excitation the assumption of $\rho_{bb} - \rho_{aa} \approx 1$ is no longer valid and we use numerical simulations to obtain $\rho(\Delta t)$. In Fig. 3 we plot $\rho(\Delta t)/\rho(0)$ obtained from Eq. (8) (with $1/\Gamma_N = 12$ ps) for weak excitation and from numerical calculations for strong excitation (pump pulse energy of 100 nJ which corresponds to the pulse area of 1.1π) and compare them with the experimental data (dots). The measured evolution of the 2^3P level population agrees with numerical and analytical calculations to the extent of the experimental precision. Such agreement indicates superradiant coherent behavior of the atomic system inside the plasma.

Coherent nature of the superradiant emission also emerged when the probe precedes the pump, as shown in Fig. 4. Some population of the 2^3P level exists prior to the arrival of the probe pulse. The probe beam creates atomic coherence between the 2^3P and 3^3D states, which lives

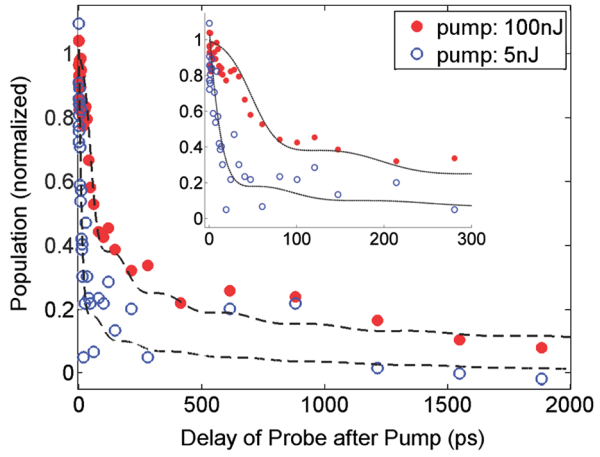

FIG. 3 (color online). Normalized population of 2^3P level as a function of time Δt after pump pulse. Dots show experimental data. Dashed curves are obtained from the analytical formula (8) with $1/\Gamma_N = 12$ ps (for weak 5 nJ pump) and by numerically solving Eqs. (1)–(4) with pump pulse area of 1.1π (for strong 100 nJ pump).

longer than the probe pulse duration. After passage of the probe pulse the coherent emission from the atomic polarization continues and contributes to the measured spectrum. Coherent emission occurs during the time of the order of the dephasing time for the atomic coherence and is called the "free-induction decay" (FID) field. When the pump pulse arrives at a delay Δt it perturbs state of the 2^3P level and, thus, modifies atomic polarization of the 2^3P-3^3D transition. This perturbation leads to the ripples in the measured spectra of transmitted probe with the period $\Delta\omega \approx 2\pi/\Delta t$. Such effect has the same origin as the "perturbed free induction decay" observed in femtosecond spectroscopy applications studying dynamics of molecules and semiconductors [9–11].

When the probe and pump pulses have temporal overlap, the transmitted probe spectrum has a clear peak at the line center of the 2^3P-3^3D transition; that is, the spectral power density at the line center is greater than that of the probe input field. This indicates that the phase of the atomic coherence between 2^3P-3^3D levels is altered by the pump in a way that leads to a free induction decay radiation in-phase with the probe at the resonance frequency of the 2^3P-3^3D transition. This is essentially the effect of cross phase modulation.

To describe the effect analytically we consider three-level system (upper level c, intermediate level a, and lower level b) and assume that at $z = 0$, the weak input probe Ω_{ca} is a Gaussian pulse with the width 2τ while the strong pump pulse Ω_{ab} has δ-function shape

$$\Omega_{ca}(t) = \Omega_{ca}^{(0)} e^{-[(t-t_{pr})/(\sqrt{2}\tau)]^2},$$

$$\Omega_{ab}(t) = \theta_{ab}^{(0)} \delta(t - t_p).$$

Here, t_{pr} (t_p) is the time that the probe (pump) pulse reaches the edge of the sample. We found that in the spectral domain the transmitted probe field has the form

$$\Omega_{ca}(\omega, L) = \Omega_{ca}^{(0)} \sqrt{2\pi}\tau e^{-i\omega(L/c+t_{pr})} \times \left\{ e^{-(\tau\omega)^2/2} - \frac{\eta L \rho_{aa}^{(0)} e^{(\Gamma_{ca}\tau)^2/2}}{\Gamma_{ca} + i\omega} \times \left[1 - |\theta_{ab}^{(0)}|^2 e^{-(\Gamma_{ca}+i\omega)(t_p - t_{pr})} \right] \right\}, \quad (10)$$

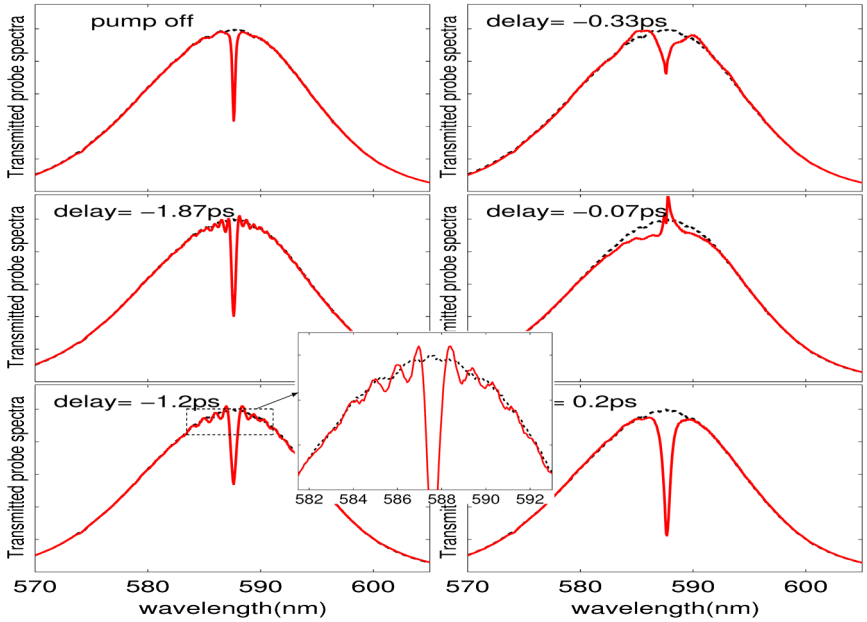

FIG. 4 (color online). Trasmitted probe spectra for different delay between probe and pump (negative delay means probe precedes the pump). The intial helium pressure before ionization is 100 mbar. Dotted lines are spectra for probe transmitted through vacuum.

where Γ_{ij} is the decoherence rate, $\omega = 2\pi(\frac{c}{\lambda} - \frac{c}{\lambda_{pr}})$, $\lambda_{pr} =$ 587 nm is the central wavelength of the probe pulse. The square of Eq. (10) gives the spectrum. The second term in the curly bracket is essentially the absorption of the probe pulse by the medium. The term $e^{-(\Gamma_{ca}+i\omega)(t_p-t_{pr})}$ shows the effect of the pump pulse which leads to the ripples with a frequency proportional to $1/(t_p - t_{pr})$, and the amplitude of the ripples decays as $e^{-\Gamma_{ca}(t_p-t_{pr})}$. When the pump pulse area is large enough, i.e., $|\theta_{ab}^{(0)}| > 1$, the spectrum will have a peak instead of a dip at the line center if the two pulses are temporally overlapping.

In summary, we observed speed up of the population decay of coherently excited helium atoms inside helium plasma. This indicates the presence of superradiant coherent emission in such system. The measured decay curve of atomic population agrees well with our analytical and numerical calculations. To best of our knowledge, our results represent the first direct probing with femtosecond transient absorption spectroscopy of the dynamics and evolution of level populations during post-ionization and recombination processes as well as direct observation on the cooperative (superradiant) decay of excited-state helium atoms with subpicosecond temporal resolution. The demonstration of laser induced coherence effects among excited states of helium prepared with optical field ionization and in medium containing helium plasma shows that coherence can play an important role in such systems that, in principle, can advance performance of plasma based XUV or x-ray sources. For example, the possibility of utilizing quantum coherence, which is key to effects like lasing without inversion, to enhance gain of XUV or x-ray lasers in He-like ions prepared via tunneling ionization has been proposed in Ref. [12]. However, effects of electron-ion collisions on atomic coherences could be crucial factors to be investigated further for successful realization of such schemes.

We thank Anatoli Morozov, Yoav Avitzour, Yushan Luo, James Mitrani, and Taehee Han for assistance in running experiment and analysis of the data, Nick Tkach for help in preparation of the experiment, and Pankaj Jha and Mikhail Shneider for helpful discussions. We gratefully acknowledge support by the National Science Foundation Physics Division Grant, the Office of Naval Research, and the Robert A. Welch Foundation (A-1261). A. S. is supported by the National Science Foundation (Award PHY-1205868). L. Y. is supported by the Herman F. Heep and Minnie Belle Heep Texas A&M University Endowed Fund. C. L. is supported by the Program in Plasma Science & Technology (PPST) at Princeton University.

[1] R. H. Dicke, Phys. Rev. **93**, 99 (1954).
[2] N. Skribanowitz, I. P. Herman, J. C. MacGillivray, and M. S. Feld, Phys. Rev. Lett. **30**, 309 (1973).
[3] G. O. Ariunbold, M. M. Kash, V. A. Sautenkov, H. Li, Y. V. Rostovtsev, G. R. Welch, and M. O. Scully, Phys. Rev. A **82**, 043421 (2010); G. O. Ariunbold, W. Yang, A. V. Sokolov, V. A. Sautenkov, and M. O. Scully, Phys. Rev. A **85**, 023424 (2012).
[4] M. Nagasono, J. R. Harries, H. Iwayama, T. Togashi, K. Tono, M. Yabashi, Y. Senba, H. Ohashi, T. Ishikawa, and E. Shigemasa, Phys. Rev. Lett. **107**, 193603 (2011).
[5] S. Suckewer and P. Jaeglé, Laser Phys. Lett. **6**, 411 (2009).
[6] L. V. Keldysh, Sov. Phys. JETP **20**, 1307 (1965).
[7] A. Egbert, D. M. Simanovskii, B. N. Chichkov, and B. Wellegehausen, Phys. Rev. E **57**, 7138 (1998).
[8] Ya. B. Zel'dovich and Yu. P. Raizer, *Physics of Shock Waves and High Temperature Hydrodynamic Phenomena* (Academic Press, New York, 1966).
[9] C. H. Brito Cruz, J. P. Gordon, P. C. Becker, R. L. Fork, and C. V. Shank, IEEE J. Quantum Electron. **24**, 261 (1988).
[10] M. Joffre, D. Hulin, A. Migus, A. Antonetti, C. Benoit à la Guillaume, N. Peyghambarian, M. Lindberg, and S. W. Koch, Opt. Lett. **13**, 276 (1988).
[11] P. Hamm, Chem. Phys. **200**, 415 (1995).
[12] E. A. Sete, A. A. Svidzinsky, Y. V. Rostovtsev, H. Eleuch, P. K. Jha, S. Suckewer, and M. O. Scully, IEEE J. Sel. Top. Quantum Electron. **18**, 541 (2012).